What Can We Still Learn from Errors?

LEIGH MCDOWELL

JALT 2021 International Conference

Research Questions

1. What are the most frequent sentence-level grammar error patterns in the research writing of Japanese materials scientists?

2. How does the identification of the most frequent sentence-level grammar error patterns affect Japanese scientists’ perceptions of errors in their own research writing?

Table 1. Overview of Corpus with Descriptive Statistics

#	Text label	Words	Sentences with errors	Errors	Errors per 1000 words
1	JR01	3,283	7	9	3
2	JR02	3,453	21	31	9
3	JR03	4,115	34	40	10
4	JR04	2,651	17	29	11
5	JR05	2,056	23	35	17
6	JR06	3,065	51	84	27
7	JR07	4,175	43	72	17
8	JR08	3,210	60	99	31
9	JR09	1,824	43	89	49
10	JR10	1,759	39	86	49
11	JR11	1,977	30	45	23
12	JR12	2,346	6	14	6
13	JR13	3,076	75	150	49
14	JR14	6,044	101	160	26
15	JR15	1,575	38	74	47
16	JR16	2,445	75	143	58
17	SR01	3,290	59	121	37
18	SR02	4,493	92	165	37
19	SR03	2,630	70	149	57
20	SR04	4,365	81	130	30
21	SR05	4,157	26	32	8
22	SR06	1,785	30	49	27
23	SR07	2,198	19	26	12
24	SR08	4,646	66	97	21
25	SR09	3,489	52	79	23
26	SR10	2,164	35	84	39
27	SR11	1,598	38	61	38
28	SR12	3,821	18	20	5
29	SR13	4,415	97	173	39
30	SR14	1,820	29	59	32
31	SR15	966	16	25	26
32	SR16	3,900	66	109	28
33	SR17	5,514	66	118	21
	Totals	**102,305**	**1,523**	**2,657**	**26**
	Min	966	6	9	3
	Max	6,044	101	173	58
	Mean	3,100	46	81	28
	SD	1,229	26	49	15

Figure 1. Thousand-word Excerpt from Corpus with Mark-up Demonstrating Average Frequency of Errors

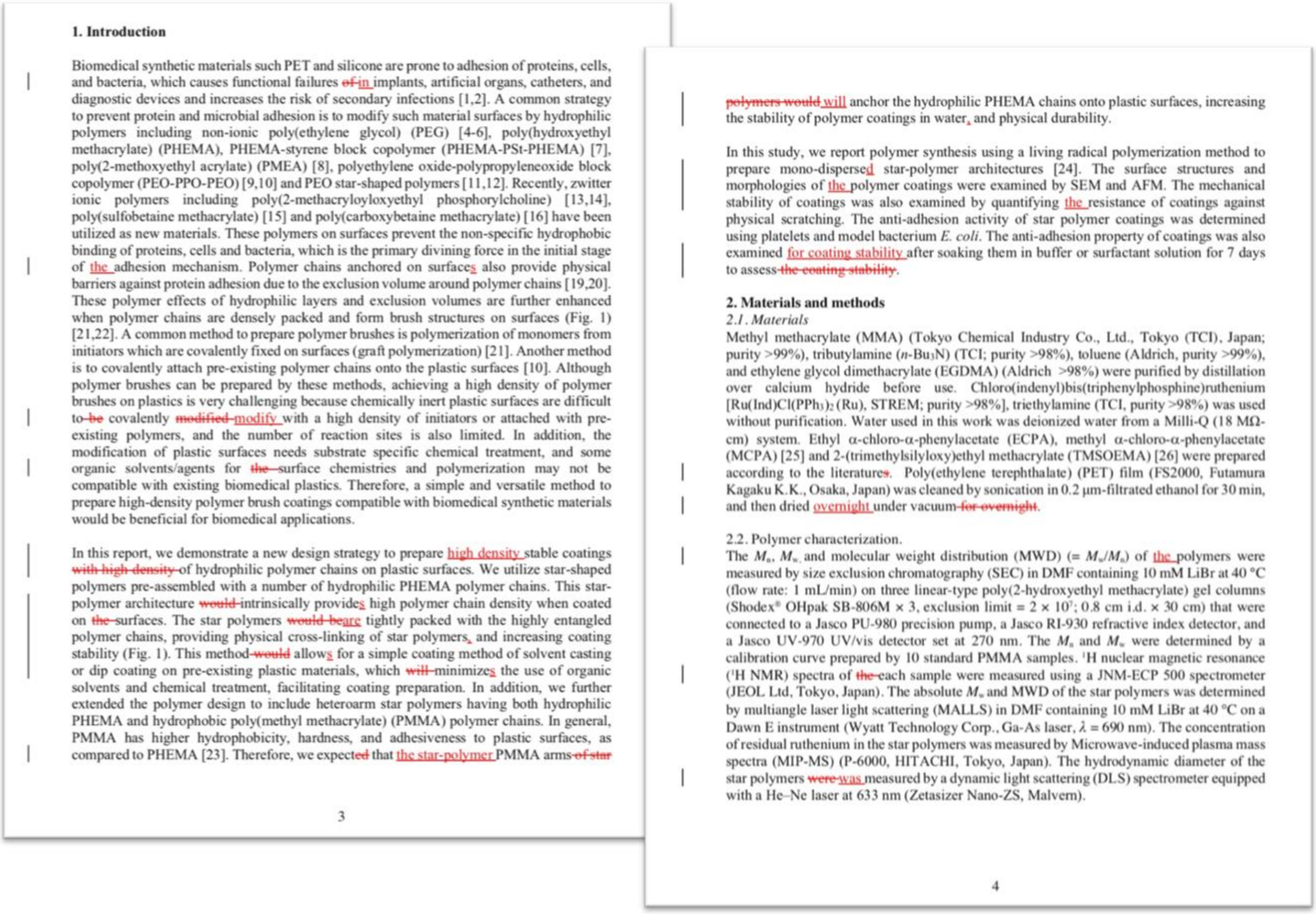

1. Introduction

Biomedical synthetic materials such PET and silicone are prone to adhesion of proteins, cells, and bacteria, which causes functional failures ~~of~~ in implants, artificial organs, catheters, and diagnostic devices and increases the risk of secondary infections [1,2]. A common strategy to prevent protein and microbial adhesion is to modify such material surfaces by hydrophilic polymers including non-ionic poly(ethylene glycol) (PEG) [4-6], poly(hydroxyethyl methacrylate) (PHEMA), PHEMA-styrene block copolymer (PHEMA-PSt-PHEMA) [7], poly(2-methoxyethyl acrylate) (PMEA) [8], polyethylene oxide-polypropyleneoxide block copolymer (PEO-PPO-PEO) [9,10] and PEO star-shaped polymers [11,12]. Recently, zwitter ionic polymers including poly(2-methacryloyloxyethyl phosphorylcholine) [13,14], poly(sulfobetaine methacrylate) [15] and poly(carboxybetaine methacrylate) [16] have been utilized as new materials. These polymers on surfaces prevent the non-specific hydrophobic binding of proteins, cells and bacteria, which is the primary divining force in the initial stage of the adhesion mechanism. Polymer chains anchored on surfaces also provide physical barriers against protein adhesion due to the exclusion volume around polymer chains [19,20]. These polymer effects of hydrophilic layers and exclusion volumes are further enhanced when polymer chains are densely packed and form brush structures on surfaces (Fig. 1) [21,22]. A common method to prepare polymer brushes is polymerization of monomers from initiators which are covalently fixed on surfaces (graft polymerization) [21]. Another method is to covalently attach pre-existing polymer chains onto the plastic surfaces [10]. Although polymer brushes can be prepared by these methods, achieving a high density of polymer brushes on plastics is very challenging because chemically inert plastic surfaces are difficult to ~~be~~ covalently ~~modified~~ modify with a high density of initiators or attached with pre-existing polymers, and the number of reaction sites is also limited. In addition, the modification of plastic surfaces needs substrate specific chemical treatment, and some organic solvents/agents for ~~the~~ surface chemistries and polymerization may not be compatible with existing biomedical plastics. Therefore, a simple and versatile method to prepare high-density polymer brush coatings compatible with biomedical synthetic materials would be beneficial for biomedical applications.

In this report, we demonstrate a new design strategy to prepare high density stable coatings ~~with high density~~ of hydrophilic polymer chains on plastic surfaces. We utilize star-shaped polymers pre-assembled with a number of hydrophilic PHEMA polymer chains. This star-polymer architecture ~~would~~ intrinsically provides high polymer chain density when coated on ~~the~~ surfaces. The star polymers ~~would be~~are tightly packed with the highly entangled polymer chains, providing physical cross-linking of star polymers, and increasing coating stability (Fig. 1). This method ~~would~~ allows for a simple coating method of solvent casting or dip coating on pre-existing plastic materials, which ~~will~~ minimizes the use of organic solvents and chemical treatment, facilitating coating preparation. In addition, we further extended the polymer design to include heteroarm star polymers having both hydrophilic PHEMA and hydrophobic poly(methyl methacrylate) (PMMA) polymer chains. In general, PMMA has higher hydrophobicity, hardness, and adhesiveness to plastic surfaces, as compared to PHEMA [23]. Therefore, we expect~~ed~~ that the star-polymer PMMA arms ~~of star~~

3

~~polymers would~~ will anchor the hydrophilic PHEMA chains onto plastic surfaces, increasing the stability of polymer coatings in water, and physical durability.

In this study, we report polymer synthesis using a living radical polymerization method to prepare mono-dispersed star-polymer architectures [24]. The surface structures and morphologies of the polymer coatings were examined by SEM and AFM. The mechanical stability of coatings was also examined by quantifying the resistance of coatings against physical scratching. The anti-adhesion activity of star polymer coatings was determined using platelets and model bacterium *E. coli*. The anti-adhesion property of coatings was also examined for coating stability after soaking them in buffer or surfactant solution for 7 days to assess ~~the coating stability~~.

2. Materials and methods

2.1. Materials

Methyl methacrylate (MMA) (Tokyo Chemical Industry Co., Ltd., Tokyo (TCI), Japan; purity >99%), tributylamine (n-Bu_3N) (TCI; purity >98%), toluene (Aldrich, purity >99%), and ethylene glycol dimethacrylate (EGDMA) (Aldrich >98%) were purified by distillation over calcium hydride before use. Chloro(indenyl)bis(triphenylphosphine)ruthenium [$Ru(Ind)Cl(PPh_3)_2$ (Ru), STREM; purity >98%], triethylamine (TCI, purity >98%) was used without purification. Water used in this work was deionized water from a Milli-Q (18 MΩ-cm) system. Ethyl α-chloro-α-phenylacetate (ECPA), methyl α-chloro-α-phenylacetate (MCPA) [25] and 2-(trimethylsilyloxy)ethyl methacrylate (TMSOEMA) [26] were prepared according to the literature~~s~~. Poly(ethylene terephthalate) (PET) film (FS2000, Futamura Kagaku K.K., Osaka, Japan) was cleaned by sonication in 0.2 µm-filtrated ethanol for 30 min, and then dried overnight under vacuum ~~for overnight~~.

2.2. Polymer characterization.

The M_n, M_w and molecular weight distribution (MWD) (= M_w/M_n) of the polymers were measured by size exclusion chromatography (SEC) in DMF containing 10 mM LiBr at 40 °C (flow rate: 1 mL/min) on three linear-type poly(2-hydroxyethyl methacrylate) gel columns (Shodex® OHpak SB-806M × 3, exclusion limit = 2×10^7; 0.8 cm i.d. × 30 cm) that were connected to a Jasco PU-980 precision pump, a Jasco RI-930 refractive index detector, and a Jasco UV-970 UV/vis detector set at 270 nm. The M_n and M_w were determined by a calibration curve prepared by 10 standard PMMA samples. ^1H nuclear magnetic resonance (^1H NMR) spectra of ~~the~~ each sample were measured using a JNM-ECP 500 spectrometer (JEOL Ltd, Tokyo, Japan). The absolute M_w and MWD of the star polymers was determined by multiangle laser light scattering (MALLS) in DMF containing 10 mM LiBr at 40 °C on a Dawn E instrument (Wyatt Technology Corp., Ga-As laser, $\lambda = 690$ nm). The concentration of residual ruthenium in the star polymers was measured by Microwave-induced plasma mass spectra (MIP-MS) (P-6000, HITACHI, Tokyo, Japan). The hydrodynamic diameter of the star polymers ~~were~~ was measured by a dynamic light scattering (DLS) spectrometer equipped with a He–Ne laser at 633 nm (Zetasizer Nano-ZS, Malvern).

4

Table 2. Excerpt from Sub-corpus of Errors Demonstrating Coding for Error Analysis

Text	Sample Sentence	Error type	Error	Re-construction	POS Error	POS Reconstruction
JR06	Cross-sectional transmission electron microscopy and Raman spectroscopy revealed that the well-dispersed and almost fully exfoliated SWNTs in PILs ~~is~~ are responsible for the enhanced thermoelectric properties.	selection	is	are	VBZ	VBP
JR06	Solid-state thermoelectrics can generate electricity with thermal-to-electric energy conversion, which has been extensively studied for ~~the~~ use in future energy resources and energy harvesting technology.	addition	the	0	DT	0
JR06	Single-walled carbon nanotubes (SWNTs) ~~have been considered as~~ are a promising candidate for future light-weight bendable thermoelectric power supply, because of their nanoporous, flexible, and highly conducting nature.	selection	have been considered	are	VHP_VBN_VVN	VBP
JR06	The relatively high electrical conductivity (*s*) of SWNTs is advantageous for large thermoelectric power generation capability which is characterized as $PF = a^2s$, where *a* is the Seebeck coefficient.	omission	0	as	0	IN
JR06	Molar extinction coefficients ~~at 409 nm~~ of oxidized K8A and K72A cyt *c* proteins at 409 nm were determined by the hemochrome method as $\varepsilon = 1.18 \times 10^5$ $M^{-1}cm^{-1}$ and $\varepsilon = 1.20 \times 10^5$ $M^{-1}cm^{-1}$, respectively.	ordering	at 409 nm	at 409 nm	IN_CD_NN	IN_CD_NN
JR06	The mixture was purified following ~~the similar~~ a manner similar to 3.	selection	the	a	DT	DT
JR06 JR06	The mixture was purified following ~~the similar~~ a manner similar to 3.	ordering	similar	similar	JJ	JJ

Table 3. Top-ten Most Frequent Error Patterns by Parts-of-speech

Rank	Error type	Error	Re-construction	Sample sentence	Frequency	Raters[*]
1	omission	0	DT	In conclusion, we have demonstrated the efficiency of the metal-ion clip method in fine-tuning aromatic stacking interactions.	503	***
2	addition	DT	0	~~The o~~Oxygen is an essential reagent in this context, however, nitrogen or water is inert to the reaction in our previous report.	244	**
3	selection	IN	IN	In this work, the mobility enhancement by the HMDS treatment or PI coating was found to be due to the increase ~~of~~ in crystalline domain size.	169	***
4	addition	IN	0	However, the tip-selective etching34 suggested by the UV-vis data could form a Se-rich surface even for the (001) face with the aid of ligand desorption ~~of ligands~~.	128	*
5	selection	NN	NNS	These different behaviors for $POCl_3$ and NO samples originated from the position where the electrons were trapped.	115	***
6	omission	0	:	The current conduction mechanisms of PA-ALD consist of SE and FNT, whereas those of T-ALD consist of SE, TAT and FNT.	107	**
7	selection	DT	DT	The DOS with SiN:F exhibited ~~the~~ a smaller value than that with SiO2 around the near conduction-band edge (Ec-E = 0.1-0.3 eV).	98	***
8	omission	0	IN	This indicates that fluorine at the interface is in an electron-rich state compared with that in the SiN:F bulk.	52	*
9	addition	RB	0	The device has a ~~very~~ compact shape.	45	*
10	selection	VBD	VBD	It appeared that the chlorophyll in the *Chlorella* cells ~~were~~ was inactivated by the plasma treatment.	31	*
				Total	1492	
				Errors/1,000 words	15	
				% of total errors	56	

[*] Asterisks indicate number of raters identifying that error pattern in their top-ten, where *** indicates three raters including the error pattern in their top-ten, ** two raters, and * one.

Figure 2. Educational Resources: Slide Series Demonstrating Top-ten Error Patterns with Field-specific Examples

1. Omission of Determiners

In order to discuss the result at higher conversion, we further examined the time course of the reaction using a high pressure mercury lamp as a light source (Table 2).

All the samples showed a typical G-band at about 1589 cm^{-1}.

A single walled CNT material (Aldrich, 50-70 % purity) with outer diameter of ca. 1.2-1.4 nm was used in this work.

2. Addition of Determiners

~~The l~~Large-diameter (> ~1.5 nm) SWNTs have unique characteristics, such as narrow band-gap and ambipolar characteristics.

The negative result obtained with LH' is ~~a~~ clear evidence that the imidazole moieties in LH acts as the distinct binding site for the second Zn2+ ion.

To get an information of the interface, a 70-nm-thick slope shape a-IGZO layer was etched using HCl (0.02 mol/l), as shown in Fig.1 (b).

3. Mis-selection of Prepositions

The obvious improvement ~~of~~ in conversion and yield under the slug flow condition even at higher conversion.

However, the 31P NMR spectra of the bicelles did not change ~~by~~ with an addition of cyt c, indicating that the bicelles maintained their structures in the presence of cyt c (Fig. S1).

At the high electric field region (E > 6~7 MV/cm), the qΦB values (2.1 eV) obtained for both T-ALD and PA-ALD are reasonable.

4. Addition of Prepositions

This enhancement in the SG-CNT Seebeck coefficient ~~of SG-CNTs~~ was then analysed from the viewpoint of dispersibility.

SG-CNTs in poly1, which were observed as white tubular shadows ~~of~~ 3 nm in diameter, form many bundles larger than 50 nm in diameter (Figure 2a).

Finally the film was dried under vacuum at 80 °C, providing round SWNT films with roughly 80 nm in thickness.

5. Mis-selection of singular noun for plural

Carbon nanotubes (CNTs) ~~is~~ are an attractive material for flexible thermoelectric devices because of their mechanical strength, lightness, and high conductivity.

To address this problem, we need to establish a new visual stimulation system that can stimulate a freely moving mouse under controlled conditions.

These optical methods measure and control complex brain function.

6. Omission of Punctuation

Thus, the desorption of ligands and etching of Cd atoms at the tips make both tips hydrophobic.

It is evident that the numbers of platelets (Figure 6B) on the coating of star-polymers, except the star-PMMA, were significantly smaller than non-coated PET.

EIS spectra in five minute intervals showed a series of shifting Nyquist plots.

7. Mis-selection of Determiners

The NRs with shorter lengths required ~~the~~ a longer aging period for self-assembly.

Transmission electron microscopy (TEM) at ~~a~~ the single-tube level revealed the existence of entangled compounds inside the SWNTs (Figure 2 (a)).

The systematic comparison enables us to conclude that the coordination geometries of (R/S)-1-5Ph in Figure 3k-t reflect the average arrangement of those in solution phase.

8. Omission of Prepositions

This indicates that fluorine at the interface is in an electron rich state compared with that in the SiN:F bulk.

More notably, the first Cotton CD band of h-PF8T2 is efficiently induced by the 546-nm irradiation, while that of l-PF8T2 is not.

Moreover, our deposition system we are able to introduce hydrogen gas during the deposition, producing a fluorinated SiNx GI layer with different hydrogen content.

9. Addition of Adverbs

The device has a ~~very~~ compact shape.

Small detergent micelles have been used for characterization of protein–lipid interactions, although a conceivable effect of the micelle curvature on the protein structure remains ~~as~~ a concern.

If the Vth definition is set to the Vgs at Id = 10-7 A, the trend of increasing DVth with increasing temperature still continues.

10. Mis-selection of past-tense *be* verbs

The in-plane thermal conductivity of SWNT buckypapers ~~were~~ was reported to be 1-10 W/mK2,29 although it is difficult to correctly determine it at the present stage.

4 and 6 was synthesized similar to 3 except for the use of 1-methylimidazole, and dehydrated pyridine.

Figure 3. Educational Resources: Field-specific Sample with Top-ten Errors (3a) Before and (3b) After Error Identification and Reconstruction

(3a)

The modern civilization has become dependent on fossil fuels of finite supply and uneven global distribution, which has two problematic consequences: (1) vulnerability of nation states to fossil-fuel imports and (2) CO_2 emissions that are acidifying our oceans and creating a global warming. The Li-ion rechargeable battery (LIB) has enabled wireless revolution of cell phones, laptop computers, digital cameras, and iPads that has transformed global communication. This technology has raised the following pressing question: Can this or another electrochemical technology enable modern civilization to secure a sustainable, distributed energy supply for all people and reduce the imprint on pollution of the air of the internal combustion engine and coal-fired power plants? A portable rechargeable battery and the electrochemical capacitor can, together, displace the internal combustion engine by powering electric vehicles, but how safely, at what cost, and over how great a driving range? Stationary rechargeable battery can store efficiently electrical energy generated by solar and/or wind power, and it can provide a distributed or a centralized energy store, but for how long a shelf and cycle life, with how rapid a response to a power outage or fluctuation of the grid, and with how large a capacity at a competitive cost?

A battery is made of one or more interconnected electrochemical cells each giving a current at a voltage for a time Δt. Here we address only issues related strategies for individual rechargeable battery cells; the management of the individual cells of a battery becomes more complex, as does the cost the larger the number of cells needed for a given battery application.

An electrochemical cell consists of two electrode, the anode and the cathode, separated by an electrolyte. The electrolyte may be the liquid or a solid. Solid electrolytes are used with gaseous or liquid electrodes; they may be used with solid electrodes, but solid–solid interfaces are problematic unless the solid electrolyte is a polymer or the solid electrodes are thin. Solid electrodes as separated by a liquid electrolyte are kept apart by an electrolyte-permeable separator.

The electrolyte conduct the ionic component of the chemical reaction between the anode and the cathode, but it forces the electronic component to traverse an external circuit where it does work.

(3b)

~~The m~~Modern civilization has become dependent on fossil fuels of finite supply and uneven global distribution, which has two problematic consequences: (1) vulnerability of nation states to fossil-fuel imports and (2) CO_2 emissions that are acidifying our oceans and creating ~~a~~ global warming. The Li-ion rechargeable battery (LIB) has enabled the wireless revolution of cell phones, laptop computers, digital cameras, and iPads that has transformed global communication. This technology has raised the following pressing question: Can this or another electrochemical technology enable modern civilization to secure a sustainable, distributed energy supply for all people and reduce the imprint on air pollution ~~of the air~~ of the internal combustion engine and coal-fired power plants? A portable rechargeable battery and the electrochemical capacitor can, together, displace the internal combustion engine by powering electric vehicles, but how safely, at what cost, and over how great a driving range? A ~~S~~stationary rechargeable battery can store efficiently electrical energy generated by solar and/or wind power, and it can provide a distributed or a centralized energy store, but for how long a shelf and cycle life, with how rapid a response to a power outage or fluctuation in ~~of~~ the grid, and with how large a capacity at a competitive cost?

A battery is made of one or more interconnected electrochemical cells each giving a current at a voltage for a time Δt. Here we address only issues related to strategies for individual rechargeable battery cells; the management of the individual cells of a battery becomes more complex, as does the cost, the larger the number of cells needed for a given battery application.

An electrochemical cell consists of two electrodes, the anode and the cathode, separated by an electrolyte. The electrolyte may be ~~the~~ a liquid or a solid. Solid electrolytes are used with gaseous or liquid electrodes; they may be used with solid electrodes, but solid–solid interfaces are problematic unless the solid electrolyte is a polymer or the solid electrodes are thin. Solid electrodes ~~as~~ separated by a liquid electrolyte are kept apart by an electrolyte-permeable separator.

The electrolyte conducts the ionic component of the chemical reaction between the anode and the cathode, but it forces the electronic component to traverse an external circuit where it does work.

Appendix A. Inter-rater reliability data

Table A1. Annotation data of errors between raters

	Sentences with errors	Errors	Errors / 1000 words	Omission	Addition	Selection	Ordering	Other
Rater 1	284	519	28	135	91	267	21	5
Rater 2	274	474	25	178	30	246	15	5
Rater 3	264	446	24	197	34	198	10	7

Table A2. Top-ten error patterns by parts of speech between raters

Rater 1				Rater 2				Rater 3			
Error type	PoS Error	PoS Re-construction	Frequency	Error type	PoS Error	PoS Re-construction	Frequency	Error type	PoS Error	PoS Re-construction	Frequency
omission	0	DT	103	omission	0	DT	76	omission	0	DT	172
addition	DT	0	35	omission	0	:	39	selection	NN	NNS	39
selection	IN	IN	30	selection	DT	DT	31	selection	IN	IN	26
selection	DT	DT	23	selection	IN	IN	26	selection	DT	DT	20
selection	NN	NNS	21	selection	NN	NNS	21	addition	DT	0	12
addition	IN	0	16	selection	NNS	NN	17	selection	TO	IN	12
addition	RB	0	13	omission	0	IN	16	selection	VBD	VBD	8
selection	RB	JJ	10	omission	0	IN/that	13	omission	0	:	7
selection	RB	RB	8	selection	TO	IN	11	ordering	RB	RB	7
selection	VBD	VBD	7	selection	VBD	VBD	10	selection	VV	VVZ	7

Appendix B. Most frequent errors

Table B1. Top-ten most frequent errors

Rank	Error type	Error	Re-construction	Sample sentence	Frequency
1	omission	0	the	In conclusion, we have demonstrated the efficiency of the metal-ion clip method in fine-tuning aromatic stacking interactions.	325
2	addition	the	0	~~The o~~Oxygen is an essential reagent in this context, however, nitrogen or water is inert to the reaction in our previous report.	194
3	omission	0	a/an	All the samples showed a typical G-band at about 1589 cm^{-1}.	176
4	addition	of	0	However, the tip-selective etching34 suggested by the UV-vis data could form a Se-rich surface even for the (001) face with the aid of ligand desorption ~~of ligands~~.	91
5	omission	0	,	The current conduction mechanisms of PA-ALD consist of SE and FNT, whereas those of T-ALD consist of SE, TAT and FNT.	83
6	selection	the	a/an	The DOS with SiN:F exhibited ~~the~~ a smaller value than that with SiO2 around the near conduction-band edge (Ec-E = 0.1-0.3 eV).	53
7	addition	a/an	0	We measured brain activities which were activated by a light fiber and a solid-state laser because we have to remove another cause of stimulation such as ~~a~~ heat and an electrical noise.	45
8	selection	of	in	In this work, the mobility enhancement by the HMDS treatment or PI coating was found to be due to the increase ~~of~~ in crystalline domain size.	36
9	selection	a	the	Therefore, multiple steps are involved until acid generation is achieved, giving rise to decomposed fragments remaining in ~~a~~ the system for these classes of PAGs.	27
10	selection	were	was	There ~~were~~ was only one hydrogen bond between the extra 310-α-310 helix and the rest of the protein, and one salt bridge between the C-terminal helix and the rest of the protein in monomeric AA cyt c555.	21